Development of High Efficiency Multi-Output Flyback Converter for Industrial Applications

Gurkan Tosun[1,3], Omer Cihan Kivanc[1,3], Ender Oguz[4], Ozgur Ustun[1,2], and R. Nejat Tuncay[1,3]

[1]Mekatro Mechatronic Systems R&D Company, ITU ARI-2 Teknokent, Istanbul, Turkey
gtosun@mekatro.com
[2]Istanbul Technical University, Istanbul, Turkey
oustun@itu.edu.tr
[3]Okan University, Istanbul, Turkey
nejat.tuncay@okan.edu.tr, cihan.kivanc@okan.edu.tr
[4]SMS-TORK Company, Istanbul, Turkey
eoguz@sms-tork.com.tr

Abstract

This study presents the development processes of a high-efficiency two-output flyback-converter. The detailed design phases are presented together with encountered design obstacles, limitations and the methods to overcome them. Despite their widely use in industry, studies on high-efficient flyback converter design still remains a need. Most of the flyback converters are designed with multi outputs for their various input voltages. This study firstly describes the preliminary design stages, modeling studies and definition of magnetic and electronic components and PCB design processes followed by a prototype manufacturing. Modelling study is conducted in MATLAB/Simulink environment, and PCB design is realized in Altium Designer Software. Prototype is tested and its performance parameters are recorded. It is seen that the performance values are good agreement with those of design objectives.

1. Introduction

It is known that, switch mode power supplies (SMPS) are widely accepted as an industrial solution for high-efficient low power applications. The weight, size, efficiency and power consumption are main constraints and objectives in designing SMPS's. In addition to small power applications, it is also used as auxiliary power sources in renewable energy systems and electric vehicles. Because of their simple topology and low cost, ease of controllability and higher voltage change ratios, the flyback converters are particularly attractive in small power industrial applications[1,2]. For example, comparatively high dc voltages of batteries in electric vehicles are converted to 12 V, 5V and 3.3V dc voltages by flyback converters. For some delicate low power industrial applications too, flyback converters are found to be attractive.

It is known that flyback dc/dc converters are derived from buck-boost topologies. Energy storing inductance in buck boost converter is replaced by a transformer, which not only provides high turns ratios but also provides the galvanic insulation. Therefore, the transformer design is one of the major tasks of designing a flyback converter. Although the importance of the snubber design is quite often underestimated, it is very important for universal flyback converters which is capable to operate in various input voltages..

In addition to their higher efficiencies, flyback converters have offer advantageous on less number of components and high reliability over the other SMPSs circuits. Besides, multiple outputs and adaptability to all single phase AC supplies (85-265 V_{AC}), step down and step up capability with a single switch explains why flyback converters are widely used in industry. [3]. Recent industrial and academic studies show that flyback converter applications are increasing in "plug and play" photovoltaic (PV) systems and multiple output applications [4, 5]. High efficiency is particularly important for PV systems. It is also possible to transfer the power grid connected flyback inverters[6]. In parallel to the expansion of photovoltaic market, the flyback converter module production is increased[6, 7, 8].

The other expanding market is the electric vehicle market, in which there is a demand for various dc voltages for auxiliary loads. This demand is fulfilled by low-cost high-efficient flyback converters[9]. These converters also provide galvanic isolation which is crucial for automotive industry and strictly defined in automotive standards.

The magnetic core and switching losses limit the flyback converter's power. It is widely used between 20-75 Watts range. The great deal degradation in efficiency occurs between 75-100 W ranges, thus a delicate design measures and special attention are necessary when designing a flyback converter in this power range. For higher power applications, single switch topologies with hard switching seems inapplicable.

The schematic circuit representation of a flyback converter is given in Fig. 1. It is known that a flyback converter operational principle is similar to that of buck-boost converter such that when switch is on the input energy is stored in magnetic circuit and then this energy inherently transferred to the load side when the switch is turned off. When switch is on, the stored energy in core is $\frac{L_p \cdot I_p^2}{2}$. When the switch is turned off, this energy transferred to the load through secondary winding and diode. It is obvious how transformer's material and its design properties, such as saturation, B-H curve of the core and even high frequency capability, are effective on the performances of the flyback converters. In any design study, without taking the above concerns, is more likely to face with some shortcomings of initial design objectives.

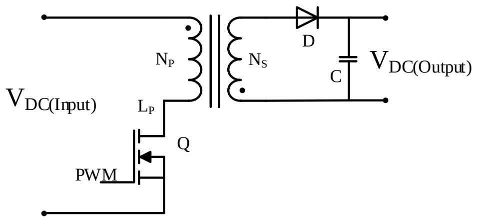

Fig. 1. Flyback converter circuit schema

Design of a flyback converter should minimize the losses and maximize the reliability. This design should also be satisfying the industrial regulations and rules. Finally a compact and reliable flyback converter with high efficiency should be manufactured. This converter must have multiple output properties and complies with universal input voltages. In the following section, all of the design stages, including component selection criteria, are described in detailed in order to reach the above objectives.

2. Design Considerations

Similar to every design and development study on SMPS circuits, this study begins with design constraints and design objectives too. These constraints and objectives mainly are: the input and output voltages, output power and voltage fluctuations, control band, efficiency, volume and weight. Since the circuit will be used in industry, the universal input voltage values (85-265 V_{AC}) are selected. Output voltage should be kept constant by satisfying the load's demand. The block representation of flyback Converter is shown in Fig. 2. The output power is defined as 90 W, which is above the load power of 81 W.

In very beginning of design study, some critical design parameters are defined initially. In addition to maximum and minimum input voltage limits, output voltage and current's maximum and minimum values, switching frequency, maximum and minimum values of duty cycle and the maximum value of output-voltage ripple-factor are among important initial design values. These values are also effective the efficiency of the device. It is known that the higher the switching frequency is lower the transformer size and weight[10]. In this study 65 kHz switching frequency is selected. This SMPS has two outputs, the voltages of them 24 V DC and 9 V dc.

Table 1. Design parameters

Parameter Description	Value
Min. Line RMS Voltage	85V AC
Max. Line RMS Voltage	265V AC
Line Frequency	50Hz
Switching Frequency	65kHz
Output Power	81W
Estimated Efficiency	90%
1st Output	24V,3A
2nd Output	9V,1A

The relationship between input and output power is given in Eq. 1, where η is efficiency and, P_{in}, P_{o1} and P_{o2} are input and two output powers respectively. P_a shows the auxiliary power output, which is negligibly low.

$$P_{in} = \frac{P_{o1} + P_{o2} + P_a}{\eta} \tag{1}$$

In order to sustain 81 W load power, all of the design studies are optimized for this value. It is no doubt, this system is capable to sustain 90 W output power continuously. In Eq.2 and Eq.3 V_{DCmin} minimum and V_{DCmax}, maximum DC input voltage equations are given. In these equations, $V_{linemin}$ and $V_{linemax}$, the maximum and minimum input voltages respectively. The D_{ch}, DC-link capacitor charging duty ratio (generally is assumed to be 0.2), C_{DC} DC link capacitor value and f_l are the line frequency. The DC bus min. and maximum voltages are calculated as, V_{DCmin}, 78V, V_{DCmax}, 375V . Since maximum supply current is required for minimum input voltage for constant demand power, the filtered dc voltage drops much lower the no load peak value. On the other hand, for the maximum input voltage case, since lowest is required for the same load, the voltage drop will almost be negligible therefore dc bus voltage could be approximated to the peak value of capacitance voltage.

$$V_{DCmin} = \sqrt{2 \cdot (V_{linemin})^2 - \frac{P_{in} \cdot (1 - D_{ch})}{C_{DC} - f_l}} \tag{2}$$

$$V_{DCmax} = \sqrt{2}\ V_{linemax} \tag{3}$$

In order to calculate the MOSFET's rated voltage, it is necessary to calculate the voltage reflected from the secondary side which is given in Eq.4, where V_{RO} reflected output voltage and D_{max}, duty cycle.

The MOSFET's rated voltage is calculated as 458 Volt by summing up the V_{RO} and V_{DCmax} voltages. In applications, it is necessary to take the transient spikes into account, thus it is advisable to use MOSFET's with rated voltages of 600 or 650 V.

$$V_{RO} = \frac{D_{max}}{1 - D_{max}} \cdot V_{DCmin} \tag{4}$$

The primary-winding inductance equation is given in Eq. 5, where P_{in} is given in Eq.1, and V_{DCmin} in Eq.2. The switching frequency f_s and max. duty cycle D_{max} are given above. In order to run the converter in *Continuous Current Mode (CCM)* under full load and minimum input voltage, $K_{RF} < 1$ is selected. Transformer primary winding inductance is obtained as L_m = 0.174 mH.

$$L_m = \frac{(V_{DCmin} - D_{max})^2}{2 \cdot P_{in} \cdot f_s \cdot K_{RF}} \tag{5}$$

When this SMPS is under full load, the peak and *RMS* value of MOSFET's current are calculated by using Eq. 6 and Eq. 7. It is obtained as, I_{dspeak} = 4.12A and I_{dsrms} = 1.83A. These values are used in selecting the MOSFET.

$$I_{ds^{peak}} = \frac{P_{in}}{V_{DCmin} \cdot D_{max}} + \frac{V_{DCmin} \cdot D_{max}}{2 \cdot P_{in} \cdot f_s} \tag{6}$$

$$I_{ds^{rms}} = \sqrt{\left[3\left(\frac{P_{in}}{V_{DCmin} \cdot D_{max}}\right)^2 + \left(\frac{V_{DCmin} \cdot D_{max}}{2 \cdot P_{in} \cdot f_s}\right)^2\right] \cdot \frac{D_{max}}{3}} \tag{7}$$

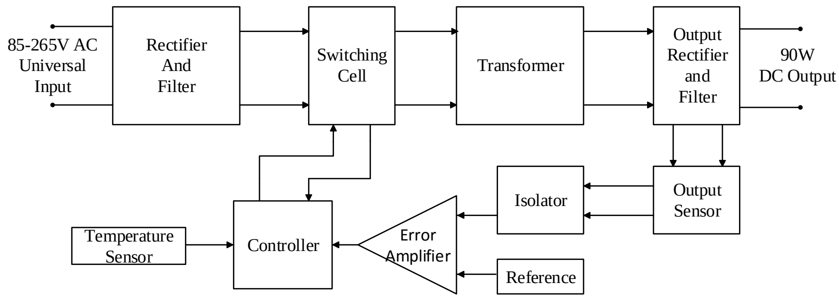

Fig. 2. Overall flyback converter block diagram

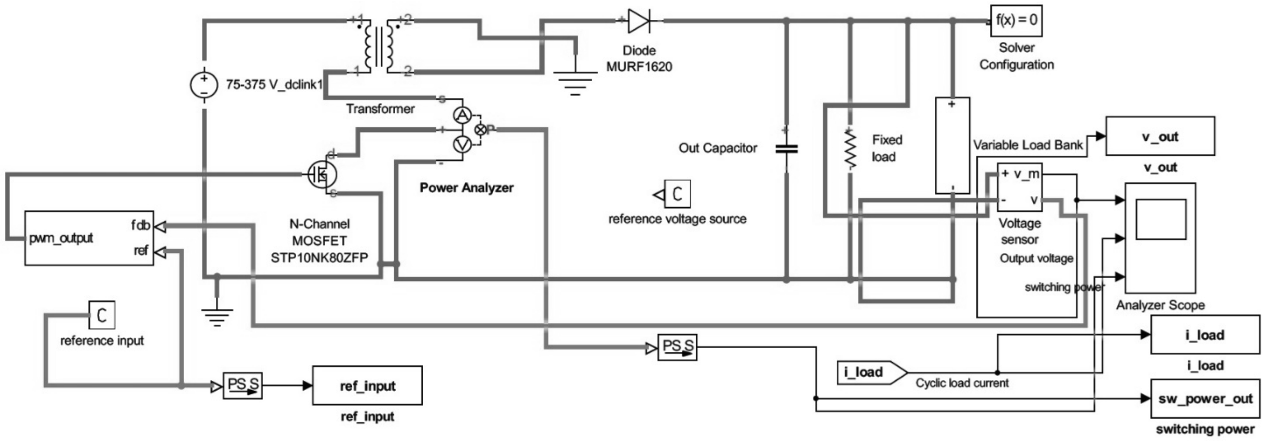

(a)

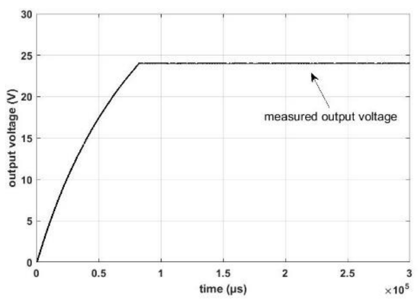

(b)

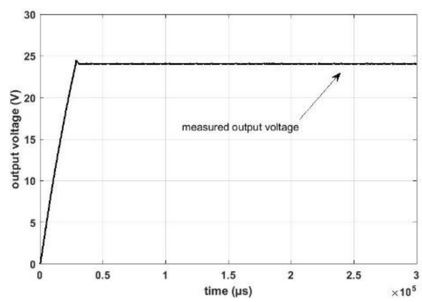

(c)

Fig. 3. Simulations with MATLAB/Simulink. (a) Flyback model in Simulink (b) Output voltage waveform for 110 V_{AC} input voltage and 3A loading (c) Output voltage waveform for 220 V_{AC} input voltage and 3A loading.

For 90W SMPS transformer, *ETD34* Core is used. The magnetic flux density and its saturated value B_{sat}, effective magnetic cross section area A_e, are used and the primary winding's minimum number of turns is obtained as 24.6. By considering the operational realities such as regulation, leakage and losses N_{pmin} = 38 is selected.

$$N_{pmin} = \frac{L_m \cdot I_{dspeak}}{B_{sat} \cdot A_e} \quad (8)$$

For either of output terminals, the secondary turns are calculated by using Eq.9 and, for 24V output N_{s1} =15 Turns and for 9V output N_{s2}= 6 Turns are calculated.

$$N_{s1} = \frac{N_p \cdot (V_{O1}+V_{F1})}{V_{RO}} \quad (9)$$

3. Simulation Results

Before starting to the PCB realization phase, simulation of the system is necessary in order to verify the calculations and optimization of the design. Simulations are done in MATLAB/Simulink environment. The block representation of SMPS model, shown in Fig. 3(a), is formed by electrical components of Simulink/SimScape library. Design parameters are tested in the simulation model and evaluated whether the calculated performance values satisfy the design objectives. In order to keep the output voltage constant, a feedback algorithm is inserted in the model. All of the operational conditions, including minimum and maximum input voltages and variable loading conditions are taken into account. As far as output voltage control is concerned, a PI controller is used and as a result of an optimization study for PI parameters, K_p=1500 and K_i=50 are obtained. In Fig. 3(a) Simulink modeling of flyback converter, in Fig. 3(b) the output-voltage waveform for 110 V_{AC} input and 3A loading, and in Fig. 3(c) the output-voltage waveform for 220 V_{AC} input and 3A loading, are shown. Simulation curves also show the system's stability and its ability to respond to load variations. The frequency response of the system is given as Bode Plots in Fig. 4. It is seen that for 180 degree phase shift, which is recommended for SMPSs, a comfortable Gain Margin is reached. Finally It should be mentioned that the design optimization study and control methodology are evaluated on the simulation model, which yields the performance values fully satisfying the design objectives.

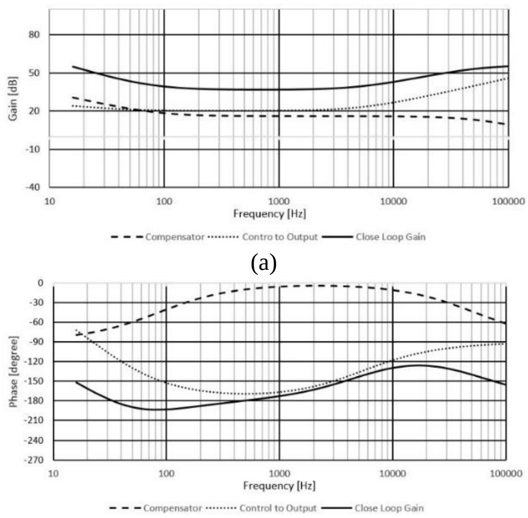

(a) (b)

Fig. 4. Bode Plots of control system

4. Manufacturing Steps of Flyback Converter

In earlier sections, the parameters affecting the design and the verification of topology and control were presented. In this section, the selection of components by considering the operational limits will be presented. The selected components are inserted in "*ALTIUM DESIGNER"* software. The circuit layout consists of five main parts, namely; AC input circuit, transformer, snubber circuit, output circuit, feedback and control circuit. In AC input side the fuses and varistors are used for protection suitable to 85-265V AC input. Additionally choke filters are used for protecting the system due to line transients. The size optimization is realized in PCB design for DC link capacitor by using three 47 µF capacitors.

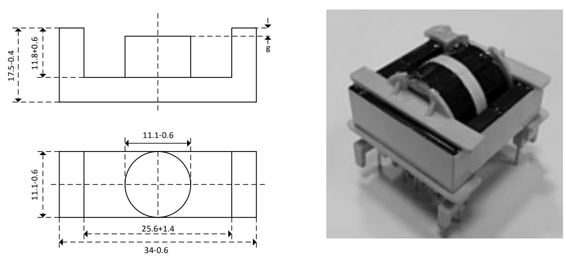

Fig. 5. The sizes and the picture of prototype transformer

The manufactured prototype transformer and its sizes are shown in Fig. 5. In order to keep the heating and cooling of transformer in optimum level, the current density is kept at approximately 7A/mm^2. In order to reduce the leakage inductance the sandwich plenary windings are designed, which provides reduction in size and power for snubber circuits and other components. It is known that the switching losses increase and efficiency reduce if the magnetizing inductance is lower[11, 12]. In this study, an extra emphasis is put on to increase the magnetizing inductance of transformer which is one of the major parameter for the efficiency of the flyback converter

For 24V and 9V outputs of the converter, rectifiers and filter capacitors are used in transformer's secondary side. Since 24V system constitutes the main power line of the system, an additional turn-off snubber circuit is added. System's 5V requirement is provided by using an output regulator.

A resistor-capacitor-diode (RCD) type snubber is used to suppress MOSFET switching. Due to the nature of flyback transformer which is having relatively higher leakage inductance, MOSFET switching can lead to excessive voltage spikes which are extremely hazardous for the switching circuit. It is a task of high importance to design a proper snubber for those types of converters. Overacting snubber circuits designed for diminishing voltage spikes entirely can be harmful instead of being useful at higher switching frequencies especially. Therefore, the design of snubber circuits for flyback converters is a highly critical task [13].

For feedback loop a voltage-to-current regulator *(TL431)* is used. This device is providing both an isolation between primary and secondary, and a filtering act which is enabling to transmit the output value to the controller precisely. The feedback loop circuit is designed by using voltage dividers which are constituting an optocoupler isolated reference current to controller through *TL431*. The feedback circuit is given in Fig. 6.

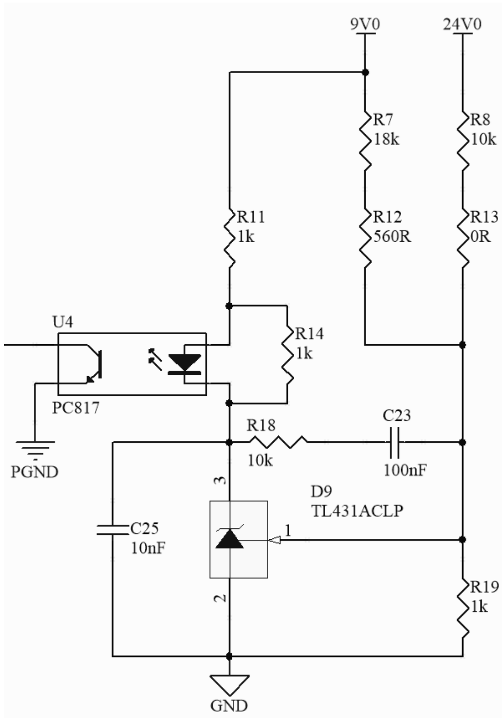

Fig. 6. Feedback circuit schematic

SG6742 IC is used for SMPS controller which is having 65 kHz switching frequency and a current feedback. An additional secondary side output is exploited to energize the controller. To start up the energizing a high voltage input in the IC receives a half-rectified input voltage from the input port through a rectifying diode and provides a momentarily 100% PWM which is enabling to transfer energy to secondary side. After this short start-up period, the controller IC is powered from the activated secondary side properly. Also a high temperature shut-down feature utilizing a temperature sensor is included in the controller [14].

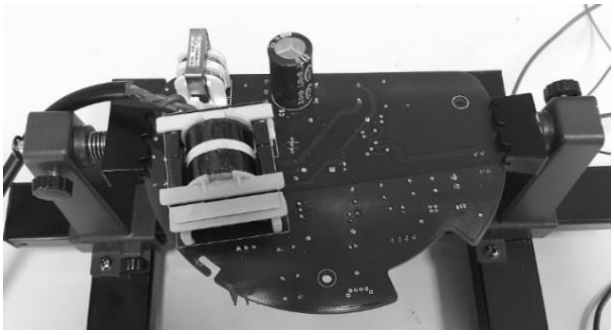

Fig. 7. Back side of the designed SMPS

The back side of the designed converter which is containing the transformer is shown in Fig. 7. In Fig. 8 the front side of the circuit is presented.

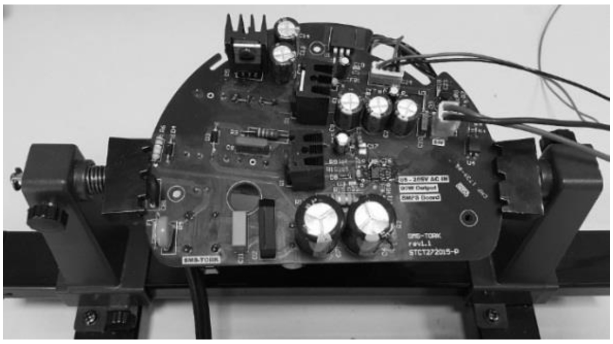

Fig. 8. Front side of the designed SMPS

5. Experimental Results

The tests of manufactured flyback converter are realized by the test system which is shown in Fig. 9. The tests are conducted for different loading and input voltage conditions. The levels of loading are accomplished by a loading bank and a variable transformer is used for changing the input voltage. A special power analyser is used for monitoring the power, efficiency and power factor.

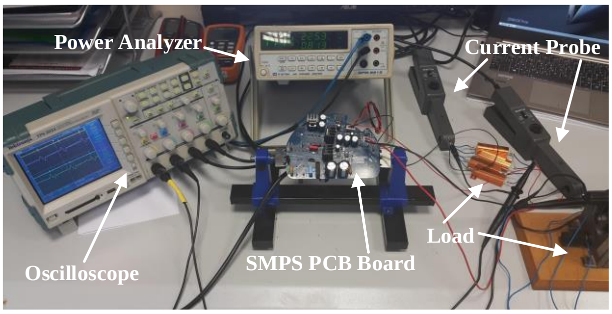

Fig. 9. Experimental test-bed

The efficiency values for different voltage inputs and fixed output power are presented in Table 2. Fig. 10 is showing the efficiency change of the converter along input voltage variation.

Table 2. Test results for constant output power

Input			Output	
Voltage [V]	**Current [A]**	**Power [W]**	**Power [W]**	**Efficiency [%]**
85,50	1,96	103,20	90,45	87,64
95,40	1,75	101,90	90,17	88,49
105,20	1,57	101,50	90,66	89,32
115,40	1,41	100,50	90,80	90,35
128,80	1,26	99,50	90,52	90,98
135,20	1,19	99,30	90,77	91,41
145,70	1,11	99,50	91,03	91,49
155,60	1,04	99,80	91,46	91,64
165,40	0,97	98,50	90,24	91,61
175,20	0,92	99,30	91,01	91,65
185,20	0,87	99,20	90,93	91,67
195,30	0,83	99,20	90,96	91,69
205,60	0,78	99,10	90,95	91,77
215,40	0,74	99,10	90,96	91,79
225,60	0,71	98,90	90,71	91,72
235,20	0,68	98,90	90,72	91,73
245,10	0,65	99,00	90,73	91,65
255,50	0,63	99,20	90,97	91,70
265,30	0,60	99,20	90,96	91,70

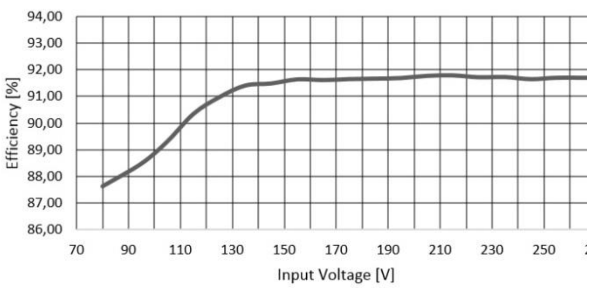

Fig. 10. Output voltage versus efficiency

In Table 3 the efficiency values for varying output power levels and fixed input voltage are given. The variation of efficiency versus output power is given in Fig. 11.

Table 3. Test results for constant input voltage

Input			**Output**	
Voltage [V]	**Current [A]**	**Power [W]**	**Power [W]**	**Efficiency [%]**
213,40	0,687	83,57	76,56	91,61
214,00	0,703	89,60	82,09	91,62
214,40	0,735	94,30	86,29	91,50
215,30	0,803	102,70	93,80	91,34
215,40	0,846	107,40	97,97	91,22
215,30	0,878	113,50	103,30	91,01
213,20	0,933	118,00	107,20	90,85

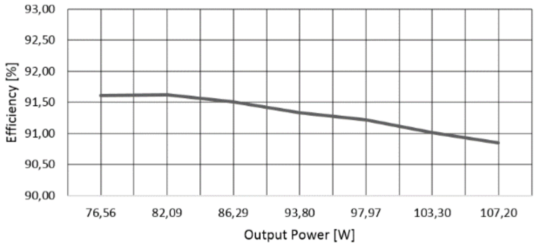

Fig. 11. Output power versus efficiency

During experimental study, the variation of output power is provided both for light loading and overloading. For increasing output powers, exceeding the rated power, the efficiency values are diminishing gradually as expected. However, as it can be seen the efficiency value is remaining at over 90% even for 20% overloading. It is concluded that these results show the validity of design.

The oscilloscope monitored output values are given in Fig. 12. The voltage and current waveforms versus time are measured for both outputs. The measurements are conducted for 90W loading. As it can be seen, all output current and voltage waveforms have the proper filtered values which can be used for energizing precise loads.

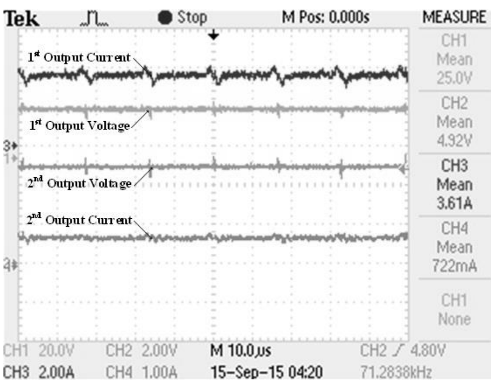

Fig. 12. Output voltage and current waveforms

In Fig. 13 gate-to-source and drain-to-source voltages of MOSFET are given simultaneously. The monitored voltages have complementary waveforms as expected. Almost there are no overlaps between two waveforms which are showing that the switching is implemented successively. The oscillations on gate-to-source voltage are denoting the behavior of snubber circuit. As it can be comprehended from the Fig. 13, a certain snubber act is to limit the voltage spike at a reasonable level. But because the losses can be increased by an overdesigned snubber some oscillating is contained.

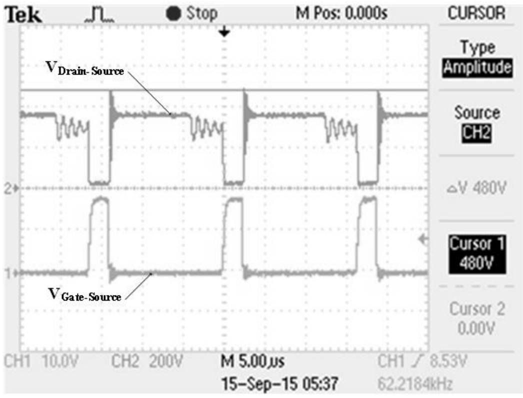

Fig. 13. MOSFET's gate voltage and drain-source voltage waveforms

6. Conclusions

In this study, all design and development stages of an industrial flyback converter are presented in detail. The implemented switch-mode converter has a wide range of input voltage and two regulated outputs. A closed loop control system is designed for keeping both output voltages constant. The circuit operation is investigated for different input and output conditions thoroughly. The obtained efficiency value is 92% which is quite suitable for industrial usage. Also the converter can be operated at some overload conditions without losing efficiency in a great deal. On the other hand, in order to aim higher efficiency values soft switching operation and energy recovering snubber features must be included in design study. However these efforts for further improving of efficiency are hindered by the fact of cost which is more essential for market oriented design solutions.

7. References

[1] T.-M. Chen and C.-L. Chen, "Analysis and design of asymmetrical half bridge flyback converter," IEE Proceedings-Electric Power Applications, vol. 149, pp. 433-440, 2002.

[2] K. Wong, "Energy-efficient peak-current state-machine control with a peak power mode," Power Electronics, IEEE Transactions on, vol. 24, pp. 489-498, 2009.

[3] J.-K. Kim and G.-W. Moon, "Derivation, Analysis, and Comparison of Non-isolated Single-Switch High Step-up Converters With Low Voltage Stress," Power Electronics, IEEE Transactions on, vol. 30, pp. 1336-1344, 2015.

[4] Q. Li and P. Wolfs, "A review of the single phase

photovoltaic module integrated converter topologies with three different DC link configurations," Power Electronics, IEEE Transactions on, vol. 23, pp. 1320-1333, 2008.
[5] F. F. Edwin, W. Xiao, and V. Khadkikar, "Dynamic modeling and control of interleaved flyback module-integrated converter for PV power applications," Industrial Electronics, IEEE Transactions on, vol. 61, pp. 1377-1388, 2014.
[6] M. Gao, M. Chen, C. Zhang, and Z. Qian, "Analysis and implementation of an improved flyback inverter for photovoltaic AC module applications," Power Electronics, IEEE Transactions on, vol. 29, pp. 3428-3444, 2014.
[7] U. Boeke, "High efficiency flyback converter technology," in 2007 Power Conversion Conference-Nagoya, 2007.
[8] Y. Hu, W. Xiao, W. Cao, B. Ji, and D. J. Morrow, "Three-Port DC–DC Converter for Stand-Alone Photovoltaic Systems," Power Electronics, IEEE Transactions on, vol. 30, pp. 3068-3076, 2015.
[9] T. Bhattacharya, V. S. Giri, K. Mathew, and L. Umanand, "Multiphase bidirectional flyback converter topology for hybrid electric vehicles," Industrial Electronics, IEEE Transactions on, vol. 56, pp. 78-84, 2009.
[10] C.-M. Wang, C.-H. Su, and C.-H. Yang, "ZVS-PWM flyback converter with a simple auxiliary circuit," IEE Proceedings-Electric Power Applications, vol. 153, pp. 116-122, 2006.
[11] B.-R. Lin, H.-K. Chiang, and C.-Y. Cheng, "Analysis and implementation of an interleaved ZVS bi-flyback converter," IET power electronics, vol. 3, pp. 259-268, 2010.
[12] B.-R. Lin, C.-E. Huang, K. Huang, and D. Wang, "Design and implementation of zero-voltage-switching flyback converter with synchronous rectifier," in Electric Power Applications, IEE Proceedings-, 2006, pp. 420-428.
[13] Muhammed H. Rashid, "Power electronics: circuits, devices & applications", Prentice Hall, New Jersey, USA, 2013.
[14] High Integrated Green-Mode PWM Controller-SG6742, IAO33.0083.B0, 2011.